Design Proposal: Mach-Zehnder Interferometer

Pongpop Sukanunta
p.sukanunta@gmail.com

I. INTRODUCTION

THE Mach-Zehnder interferometer (MZI) serving as a fundamental building block for filtering, switching, and phase-modulation functions. This proposal investigates the design and analysis of MZIs by first characterizing the waveguide geometries through mode simulations. A compact model is then contructed to enable efficient circuit-level simultion in Lumerical INTERCONNECT. Different path-lenght differences of the unbalanced MZI are evaluated and compared for their free spectral range (FSR) and transmission.

II. THEORY

A. Transfer Function of an MZI

The Mach-Zenhder interferometer (MZI) operates by splitting an input light into two paths and then recombining them at the output. The splitting and combinging can be done with many means. For this design, we are using Y-branches with $50/50$ power ratio for both of the spliter and the combiner. The schematic of an MZI is shown in figure 1.

Considering the first Y-Branch, an input field E_i is splitted equally into $E_{i1} = E_{i2} = E_i/\sqrt{2}$. The two branches have length L_1 and $L_2 = L_1 + \Delta L$. The propagation in each waveguide is described by $\beta_1 = \frac{2\pi n_1}{\lambda}$ and $\beta_2 = \frac{2\pi n_2}{\lambda}$, where n_1 and n_2 are the effective indices of the respective waveguides. Negecting loss in the waveguide, the field at the combiner are

$$E_{o1} = E_{i1}e^{-i\beta_1 L_1} = \frac{E_i}{\sqrt{2}}e^{-i\beta_1 L_1} \tag{1a}$$

$$E_{o2} = E_{i2}e^{-i\beta_2 L_2} = \frac{E_i}{\sqrt{2}}e^{-i\beta_2 L_2} \tag{1b}$$

The second Y-branch recombines these fields, giving the output field

$$E_o = \frac{E_{o1} + E_{o2}}{\sqrt{2}} = \frac{E_i}{2}\left(e^{-i\beta_1 L_1} + e^{-i\beta_2 L_2}\right) \tag{2}$$

The corresponding output intensity is

$$I_o = \frac{I_i}{4}\left|e^{-i\beta_1 L_1} + e^{-i\beta_2 L_2}\right|^2 \tag{3}$$

$$= \frac{I_i}{2}\left[1 + \cos\left(\beta_1 L_1 - \beta_2 L_2\right)\right] \tag{4}$$

In case of identical waveguides, this simplifies to the well-known MZI transfer function

$$I_o = \frac{I_i}{2}\left[1 + \cos\left(\beta\Delta L\right)\right] \tag{5}$$

Fig. 1. Schematic of a Mach-Zanhder Interferometer

B. Free Spectral Range of MZI

Equation 5 shows that an unbalanced MZI produces a periodic spectral response. The wavelength spacing between adjacent peaks is the free spectral range (FSR); FSR $= \Delta\lambda = \lambda_m - \lambda_{m+1}$. A full period occurs when the phase difference increases by 2π:

$$2\pi = \beta_m \Delta L - \beta_{m+1}\Delta L \tag{6a}$$

$$2\pi = \left(\beta_m - \beta_{m+1}\right)\Delta L \tag{6b}$$

$$\Delta\beta = \frac{2\pi}{\Delta L} \tag{6c}$$

β can be approximate to varies linearly with λ

$$\Delta\beta \approx -\frac{d\beta}{d\lambda}\Delta\lambda \tag{7}$$

Substituting into Eq. 7, Equation 6c becomes

$$-\frac{d\beta}{d\lambda}\Delta\lambda = \frac{2\pi}{\Delta L} \tag{8a}$$

$$\Delta\lambda = -\frac{2\pi}{\Delta L}\left(\frac{d\beta}{d\lambda}\right)^{-1} \tag{8b}$$
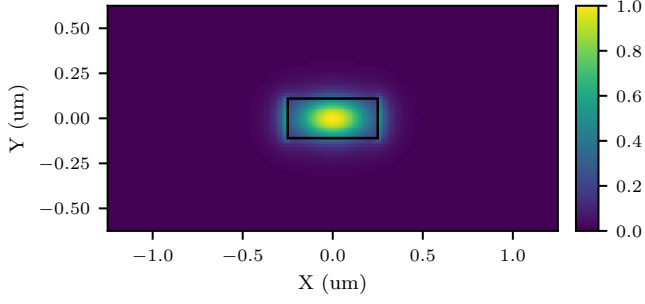
Since $\beta = \frac{2\pi n}{\lambda}$, the free spractral range becomes:

$$\text{FSR} = \frac{\lambda^2}{\Delta L\left(n - \lambda\frac{dn}{d\lambda}\right)} \tag{9}$$

$$= \frac{\lambda^2}{\Delta L n_g} \tag{10}$$

where n_g is the group index,

$$n_g = n - \lambda\frac{dn}{d\lambda} \tag{11}$$

Fig. 2. Simulated profile of the TE$_0$ mode.

TABLE I
SUMMARY OF SIMULATED WAVEGUIDE PARAMETERS.

Parameter	Value
Core material	Si
Cladding material	SiO$_2$
Waveguide width	500 nm
Waveguide height	220 nm
Polarization	TE$_0$
Wavelength range	1500–1600 nm

III. MODELLING AND SIMULATION

A. Waveguide

Lumerical MODE's eigenmode solver was used to characterize the waveguide structure. The simulated device is a silicon strip waveguide with a 220 nm silicon core thickness and a width of 500 nm, embedded in a silicon dioxide cladding. A summary of the waveguide parameters used in the simulations is provided in Table I.

The fundamental TE$_0$ mode profile at the design wavelength is shown in figure 2. A wavelength sweep from 1500 nm to 1600 nm was performed. The wavelength-dependent effective index and group index extracted from the eigenmode simulations are shown in figure 3 and figure 4, respectively.

To enable efficient circuit-level simulations, a waveguide's compact model was constructed by fitting the simulated effective index to a second-order Taylor expansion around a reference wavelength λ_0. The compact model has the form

$$n_{eff}(\lambda) = n_1 + n_2(\lambda - \lambda_0) + n_3(\lambda - \lambda_0)^2 \qquad (12)$$

The fitted coefficients are summarized in Table II, and the resulting compact model is compared with the numerical MODE data in figure 5.

B. MZI circuit

The MZI circuits were modeled and simulated using the EBeam compact model provided in the SiEPIC-EBeam-PDK

TABLE II
FITTED COEFFICIENTS OF COMPACT MODEL.

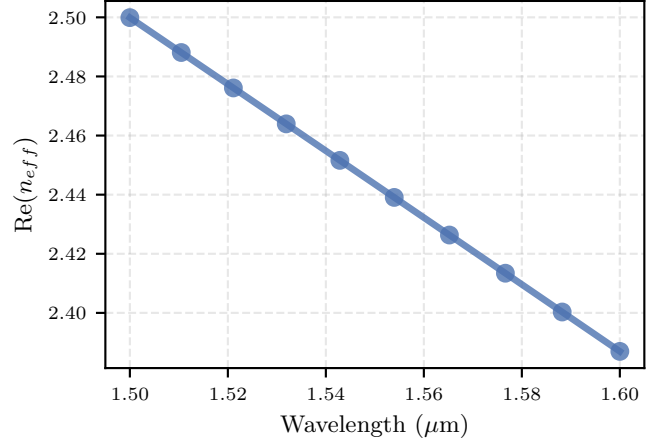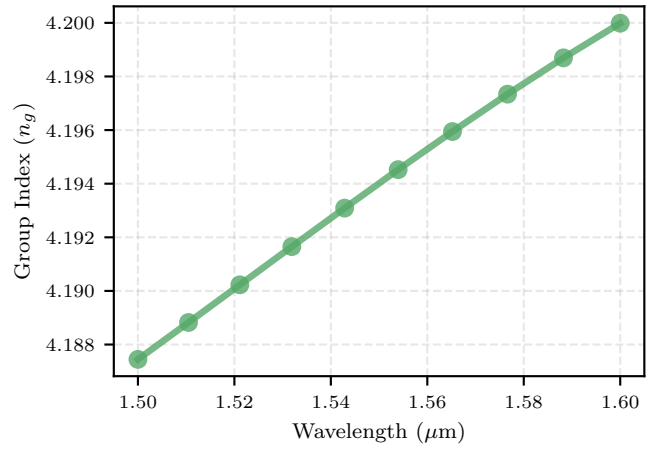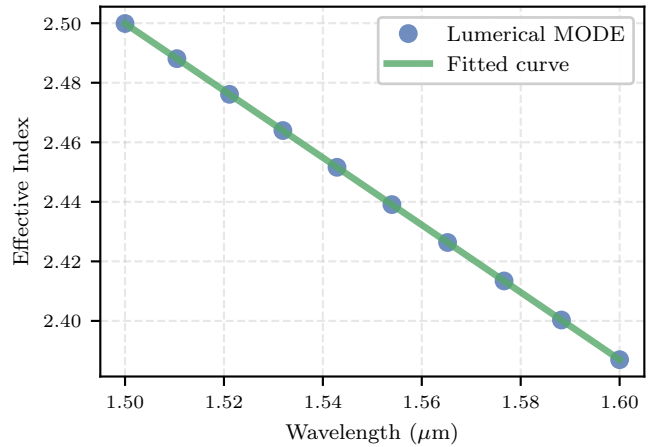| Coefficient	Value
n1	2.444
n2	-1.129
n3	-0.041

Fig. 3. Simulated fundamental TE-mode effective index $n_{eff}(\lambda)$.

Fig. 4. Simulated fundamental TE-mode group index $n_g(\lambda)$.

Fig. 5. Comparison between the simulated effective index and the second-order compact model fitted around the reference wavelength.

and implemented in Lumerical INTERCONNECT. The MZIs are model and simulated using the EBeam compact model from SiEPIC-EBeam-PDK in Lumerical INTERCONNECT.

TABLE III
EXPECTED FSR FROM PATH DIFFERENCE ΔL.

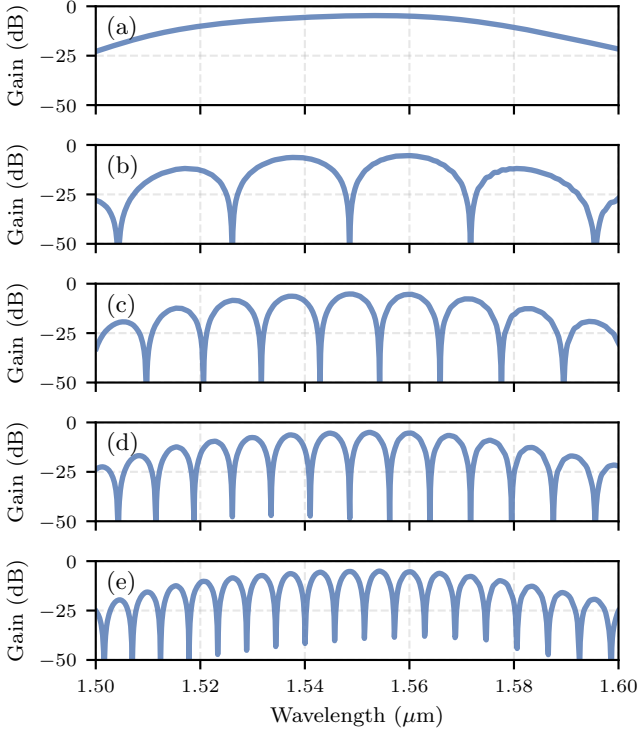| ΔL (μm)	FSR (nm)
25	22.91
50	11.46
75	7.64
100	5.73

Fig. 6. (a) Grating-coupler insertion loss reference spectrum. (b-e) MZI transmission for path-length differences $\Delta L = 25, 50, 75, 100$ μm, respectively.

Fig. 7. Complete GDS layout of the designed photonic chip. For the actual gds layout see `EBeam_Pongpop.gds`.

The main design parameter for an unbalanced MZI is the differential path length ΔL, which directly determines the FSR.

A set of MZIs with different ΔL values was simulated to evaluate the resulting FSR. Table III summarizes the ΔL and their corresponding predicted FSRs using equation 9.

Each MZI was then simulated in INTERCONNECT using wavelength-domain sweeps from 1500-1600 nm. The simulated TE-mode transmission responses is shown in figure 6, including the insertion loss from the grating coupler. The circuit-level layout generated fr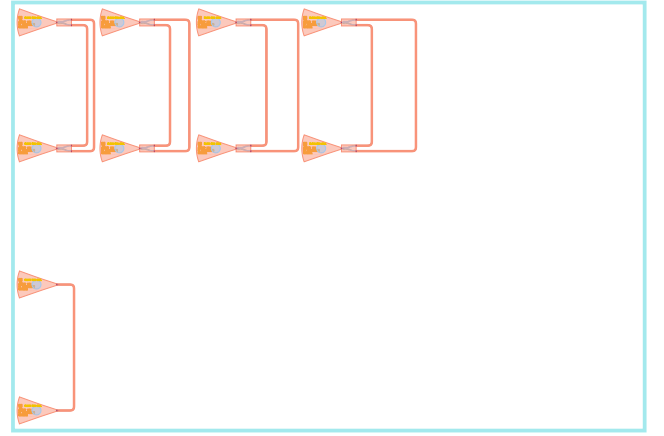om the SiEPIC PDK components is shown in figure 7.